

Supporting information

Inversion of crystallization rates in miscible block copolymers of poly(lactide)- block-poly(2-isopropyl-2-oxazoline)

Fabian Pooch,^a Marjolein Sliepen,^a Kirsi J. Svedström,^b Antti Korpi,^c Françoise M. Winnik,^{a,d,e} Heikki Tenhu^{*a}

^a Department of Chemistry, University of Helsinki, P.O. Box 55, Helsinki 00014, Finland

^b Department of Physics, University of Helsinki, P.O. Box 64, Helsinki 00014, Finland

^c Department of Bioproducts and Biosystems, Aalto University, P.O. Box 16100, Aalto 00076, Finland

^d WPI International Centre for Nanoarchitectonics (MANA), National Institute for Materials Science (NIMS), 1-1 Namiki, Tsukuba 305-0044, Japan

^e Département de Chimie, Université de Montréal, CP 6128 Succursale Centre Ville, Montréal QC H3C 3J7, Canada

* corresponding author (E-mail: heikki.tenhu@helsinki.fi)

Contents:

- 1) *Polymer characterization*
- 2) *Calculation of solubility parameters*
- 3) *T_g regions of all BCPs*
- 4) *Detailed crystallization properties of the homopolymers*
- 5) *Isothermal crystallization of 2L3*
- 6) *Isothermal crystallization raw data*
- 7) *References*

1) Polymer characterization

1.1) Characterization of PiPOx homopolymers

Cationic ring-opening polymerization (CROP) of oxazolines belongs to the family of living polymerizations.² This was confirmed experimentally by the linear evolution of $-\ln(1 - X_p)$ vs. time,

Supporting information

where X_p is the conversion determined by $^1\text{H-NMR}$ and by plots of M_n vs. X_p (Figure S2). The rate of polymerization (k_p) increased linearly with the initiator concentrations. The dispersity of the purified PiPOx ranged between 1.08 and 1.28 according to SEC. The molecular weights were determined by MALDI-TOF, SEC and $^1\text{H-NMR}$ spectroscopy and compared to their theoretical values (Table S1). MALDI-TOF (Figure S1 A) gave the best match to the theoretical molecular weights. The MALDI-TOF spectrum of Ox^{15.5} showed some tailing on the low molecular weight side. This is believed to be an artefact, since the SEC trace of this polymer was symmetrical and narrow (Figure S1 A, inset). The fine structure of the MALDI-TOF spectrum of Ox^{2.0} (Figure S1 B) revealed the presence of four different polymeric species for each n-mer (n: degree of polymerization, blue numbers). These species were separated from their (n + 1) analogs by the weight of one repeating unit (113 g/mol). For each n-mer, the two peaks with highest intensity originated from Me-PiPOx_n-N₃ and Me-PiPOx_n-N, the latter being a metastable post-source ion after expulsion of N₂ due to the high laser power of the instrument.³ The two peaks of lower intensity correspond to H-PiPOx-N₃ and H-PiPOx-N. These species are products of proton initiation.⁴ As all the species originate from azide terminated polymers, one can conclude based on the MALDI-TOF spectra that the termination of the polymerization with azide-groups was quantitative.

Table S1 Polymerization conditions and characterization of PiPOx and PLA homopolymers

Polymer	[M]/[I]	X_p	t / h	$M_{n,theo}^a$	$M_{n,NMR}^a$	$M_{n,SEC}^a$	$M_{n,MALDI}^a$
PiPOx1	26	0.74	5	2.2	2.8	2.0	2.1
PiPOx2	74	0.8	18	6.7	11.6	9.3	7.1
PiPOx3	132	0.76	43	11.4	28.8	15.5	12.5
PLLA1	19	0.98	1.5	2.7	2.7	5.9	-
PLLA2	38	0.98	1.5	5.4	5.3	10.0	-
PLLA3	77	0.97	1.5	10.8	8.9	14.6	-
PDLA1	19	0.98	1.5	2.7	3.3	4.9	-
PDLA2	32	0.97	1.5	4.5	5.1	9.0	-
PDLA3	71	0.96	1.5	9.8	10.8	17.7	-

^a in kg/mol;

Supporting information

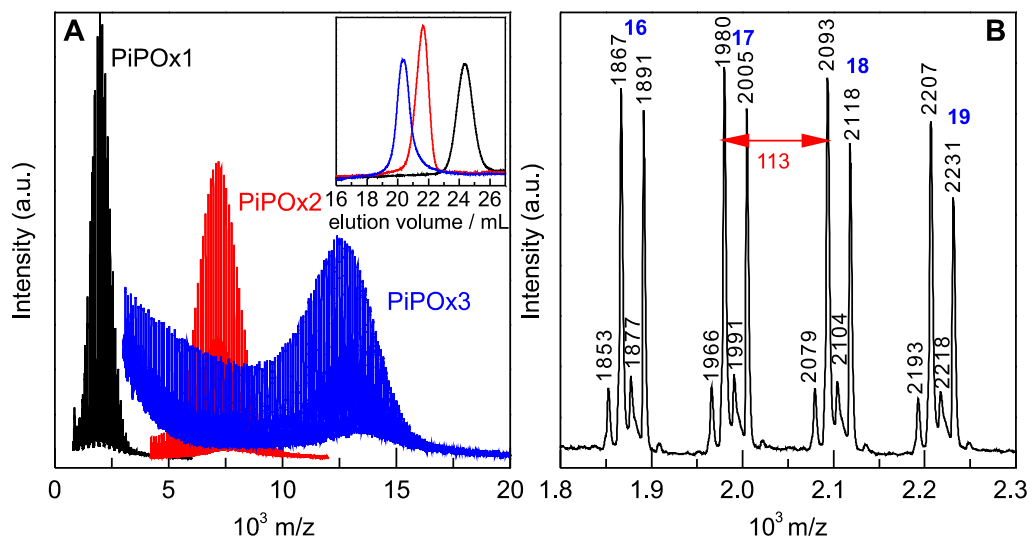


Figure S1 MALDI-TOF spectra of the three PiPOx homopolymers (A), and a zoom into the spectrum of Ox^{2.0} (B). The inset of (A) shows the SEC traces of the respective polymers.

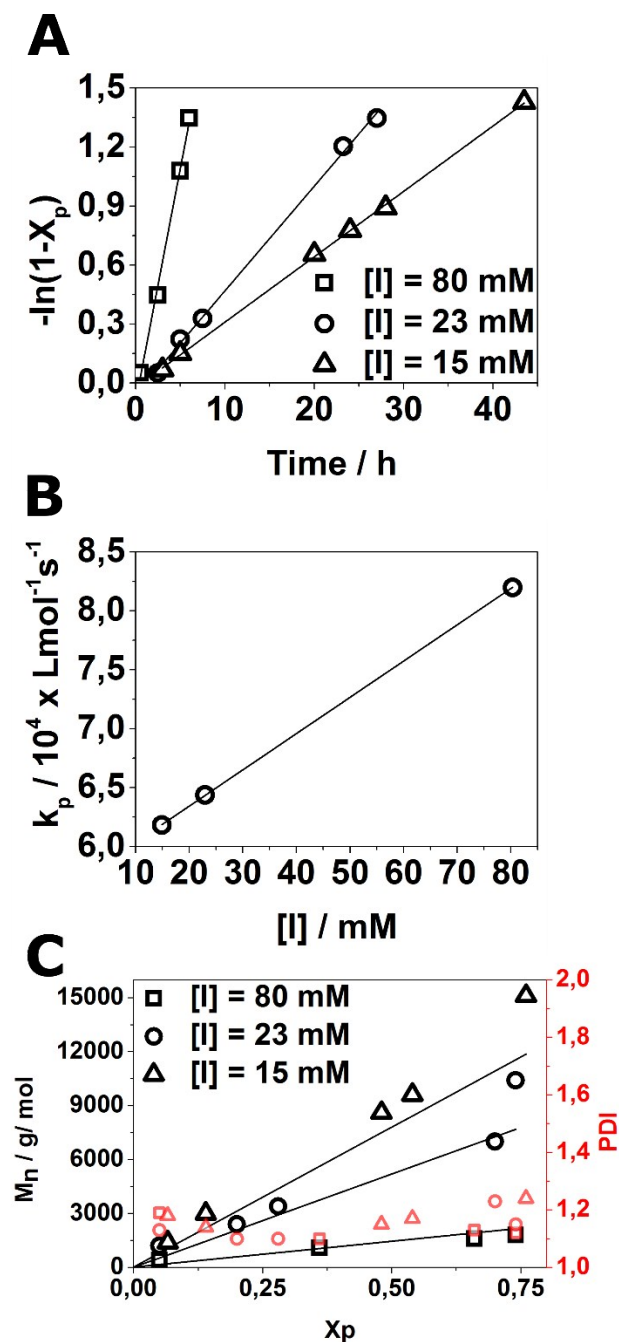


Figure S2: Kinetics of the polymerization of iPOx in acetonitrile ($[iPOx]_0 = 28 \text{ wt\%}$; $T = 70 \text{ }^\circ\text{C}$). (A) Time vs $-\ln(1-X_p)$ plot for different initiator concentrations, (B) rate constants as a function of initiator concentration, (C) development of molecular weight and dispersity with increasing conversion X_p .

1.2) Characterization of PLA homopolymers

The PLA homopolymers were synthesized by bulk polymerization of L- or DL-lactide using tin octanoate as catalyst and propargyl alcohol as initiator. This procedure yielded PLA homopolymers with α -

Supporting information

propargyl and ω -hydroxyl groups. In view of the melting points of the monomers, the polymerizations of L-lactide and DL-lactide were conducted at 110 °C and 130 °C, respectively. The molecular weights were controlled by adjusting the lactide-to-propargyl alcohol ratio. Theoretical molecular weights and end-group analysis by $^1\text{H-NMR}$ spectroscopy were in good agreement (Table 1). In contrast, SEC (Figure S2) overestimated the molecular weights by a factor of up to 2, which is well known.⁵ All $^1\text{H-NMR}$ spectra of the PLA homopolymers showed signals at 2.50 and 4.72 ppm (Figures S3 and S4) originating from the α -propargyl protons. In general, PLLA homopolymers had a narrower PDI than PDLLA homopolymers.

1.3) Characterization of the BCPs

The coupling reactions were conducted with an excess of PiPOx (1.2 eq) in order to achieve complete conversion of PLA propargyl-groups. The unreacted excess PiPOx was removed by dispersing the dried crude mixture in water, followed by centrifugation. The BCP was recovered from the pellet. The supernatant contained excess PiPOx which readily dissolves in cold water. Comparison of the SEC traces of crude and purified BCPs (Figure S4) confirmed that unreacted PiPOx was successfully removed. The $^1\text{H-NMR}$ spectra of the BCPs did not display the original propargyl signals (signals F and I, Figures S3 and S4). Four new proton signals corresponding to PiPOx- $\text{CH}_2\text{-CH}_2\text{-triazole-CH-C-CH}_2\text{-PLA}$ (Figure S3, signals D', D'', F', and I') were observed at 3.16, 3.87, 7.60 and 4.62 ppm, respectively. The integration of these new signals and that of the signals due to the two end-groups at 3.06 and 4.38 ppm (signals C and H, respectively) were consistent with the expected numbers of protons.

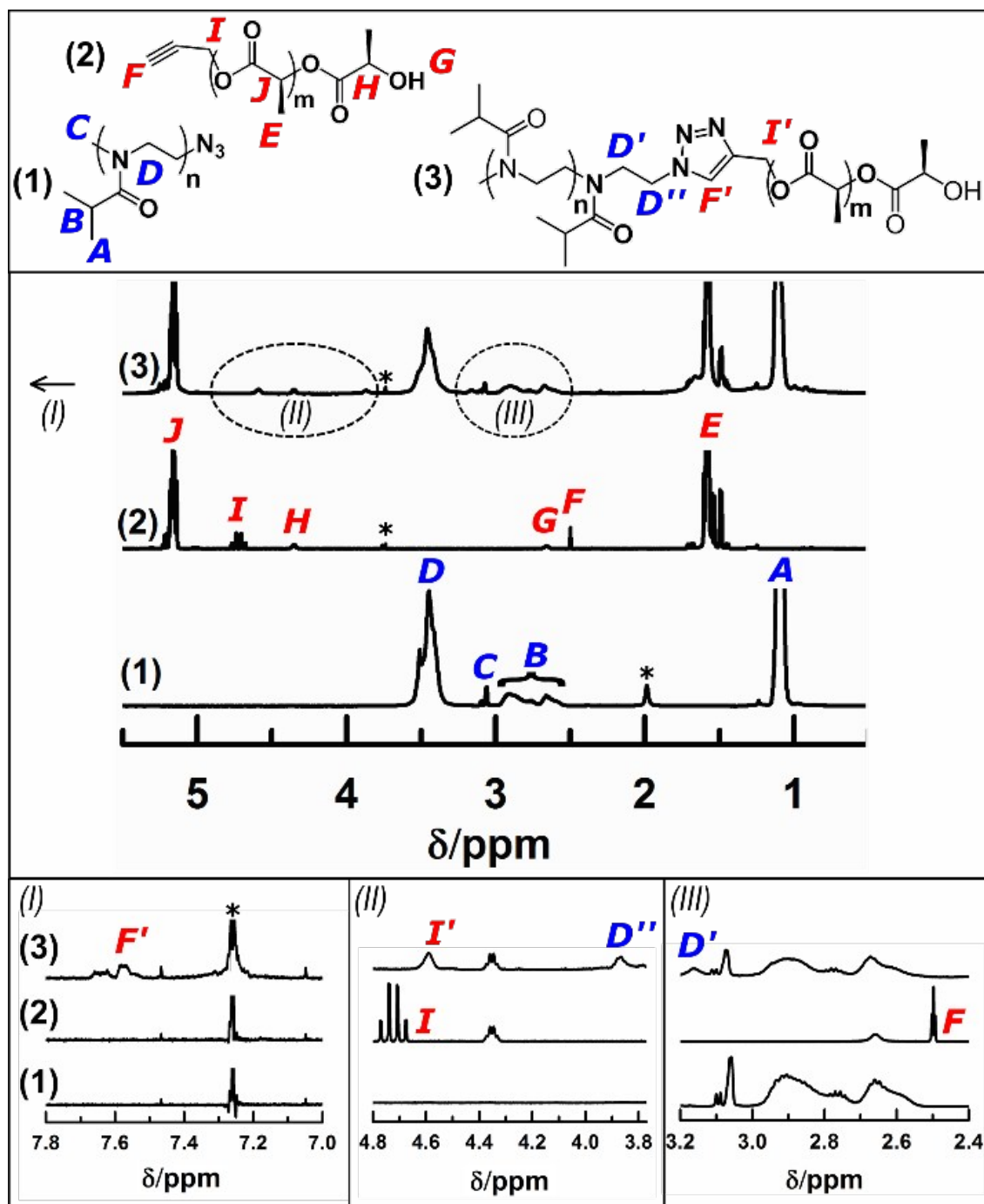
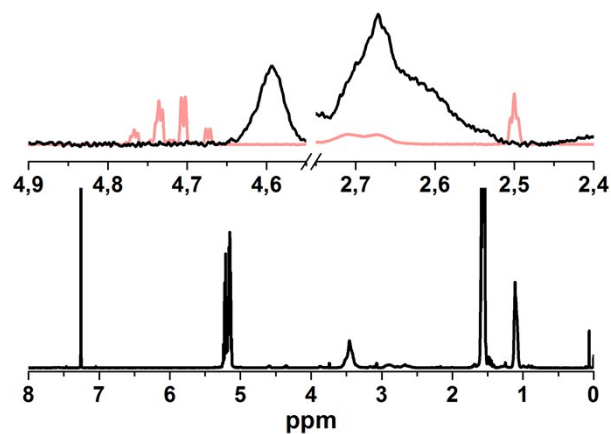
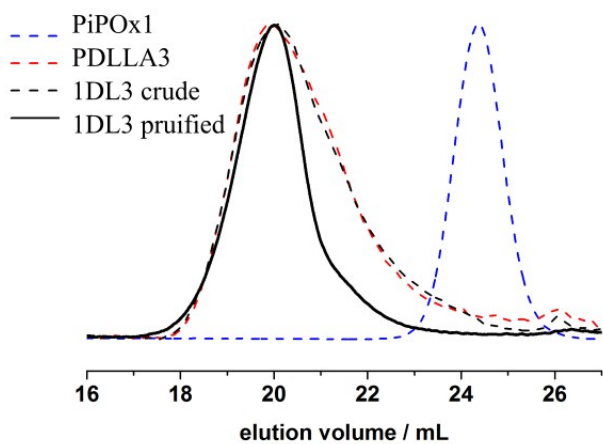
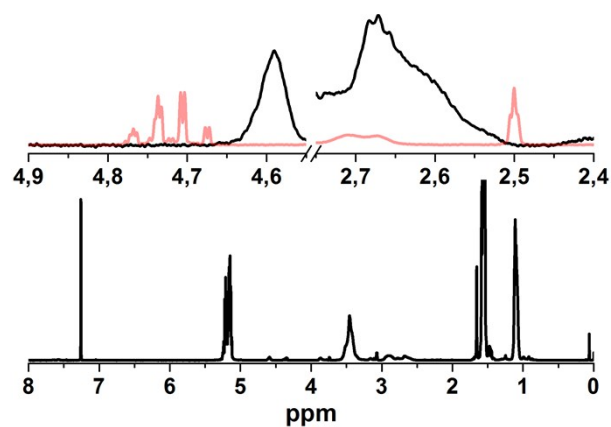
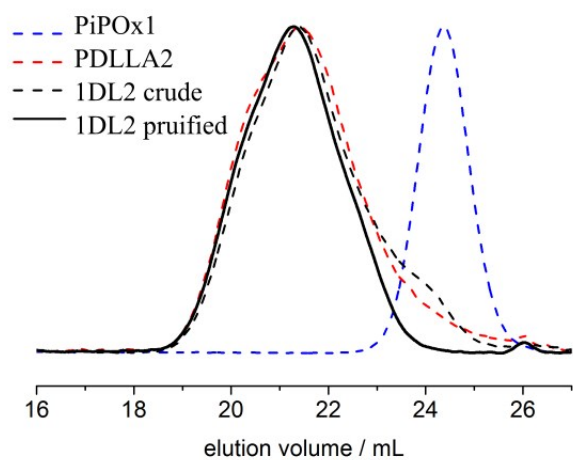
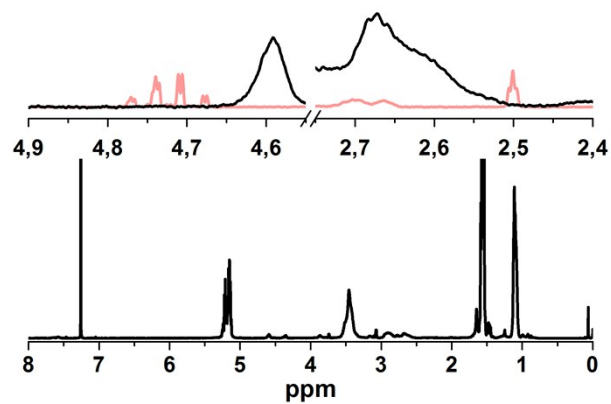
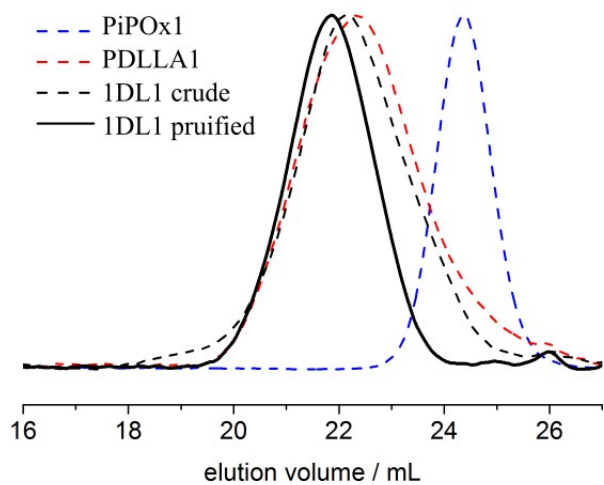
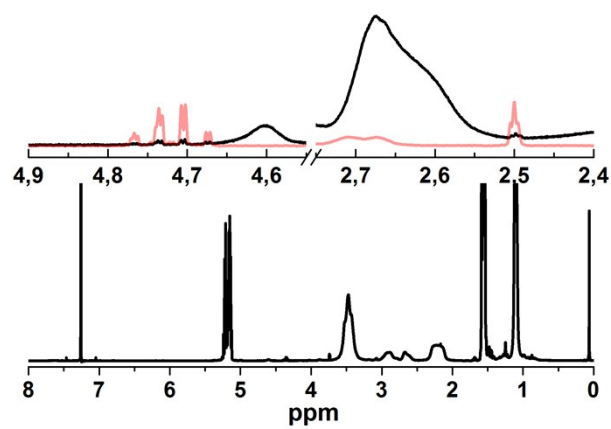
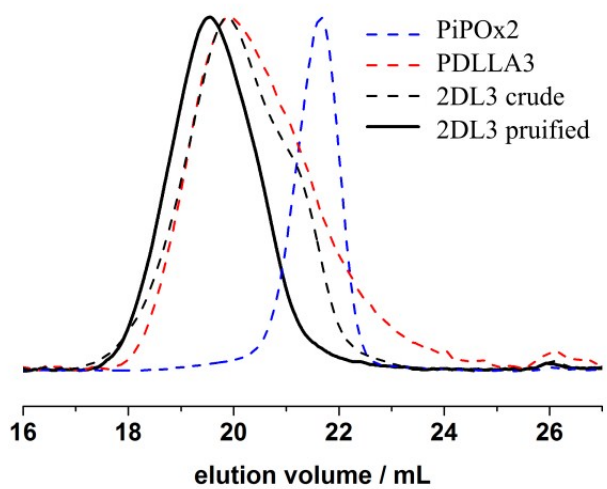
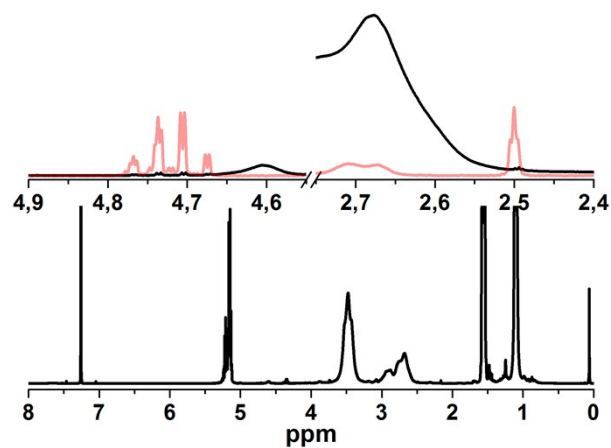
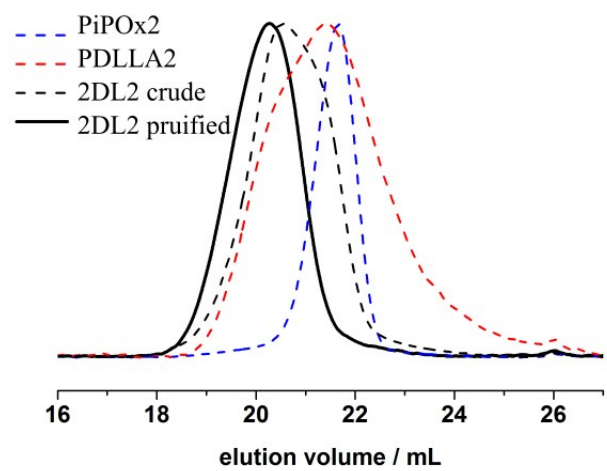
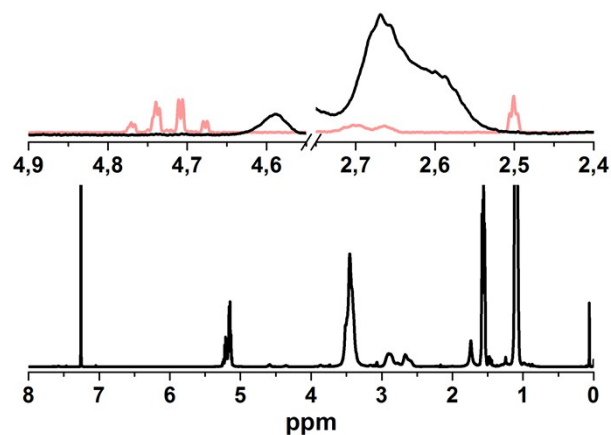
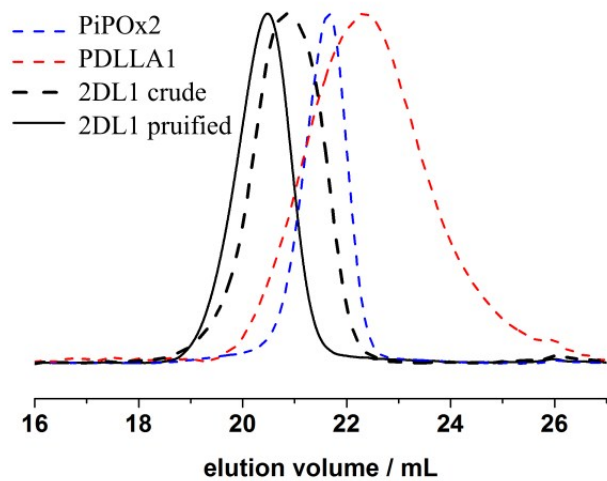


Figure S3 Chemical structures and $^1\text{H-NMR}$ spectra (CDCl_3) of PiPOx1 (1), PLLA1 (2) and 1L1 (3). In the structure and spectrum of (3) only the signals with altered chemical shift are pointed out. Note the disappearance of the original propargyl signals F and I in the BCP. Asterisks mark residual 1,4-dioxane.

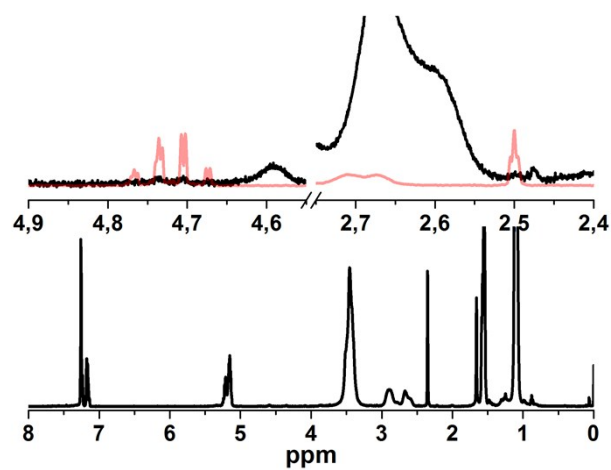
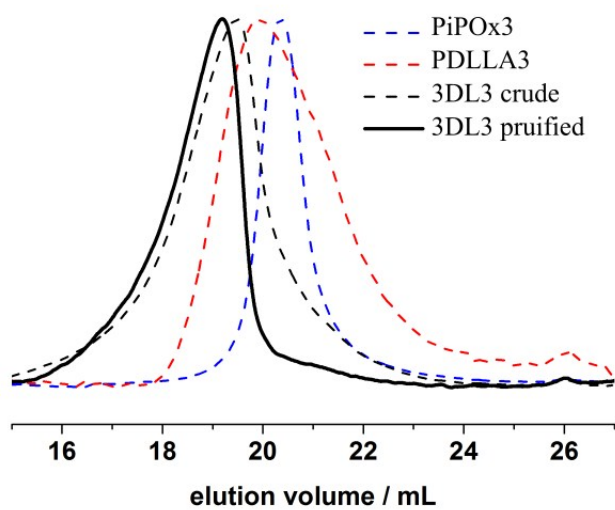
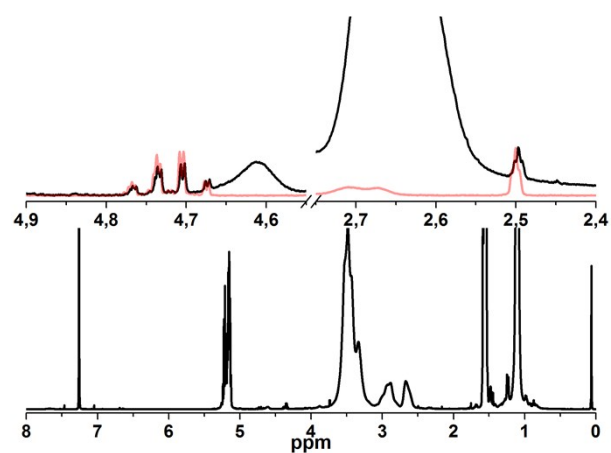
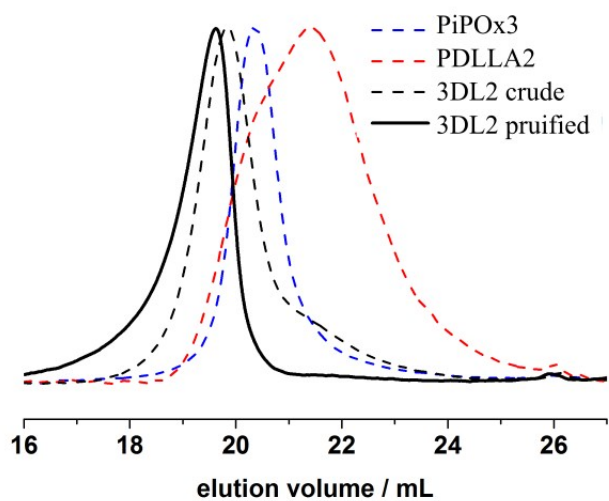
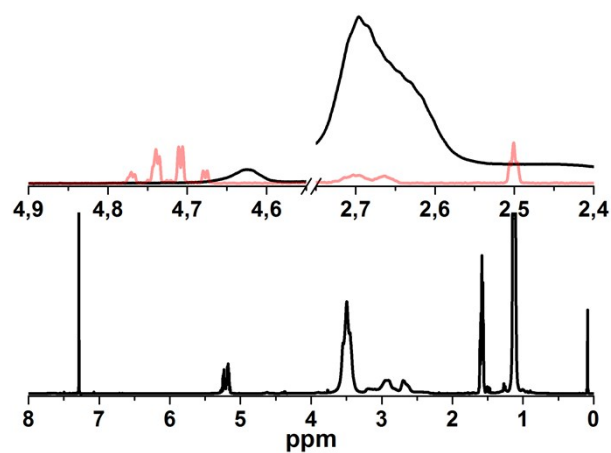
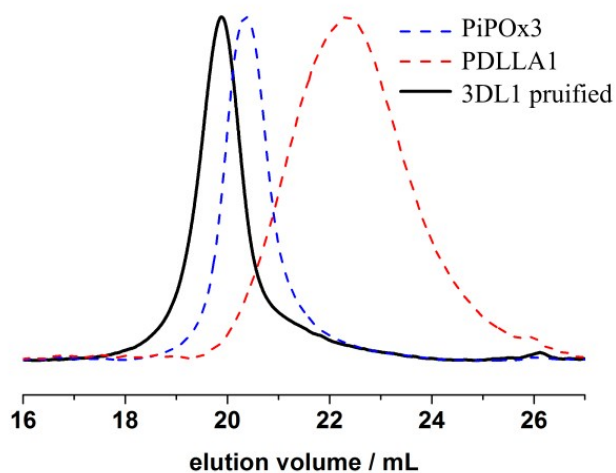
Supporting information



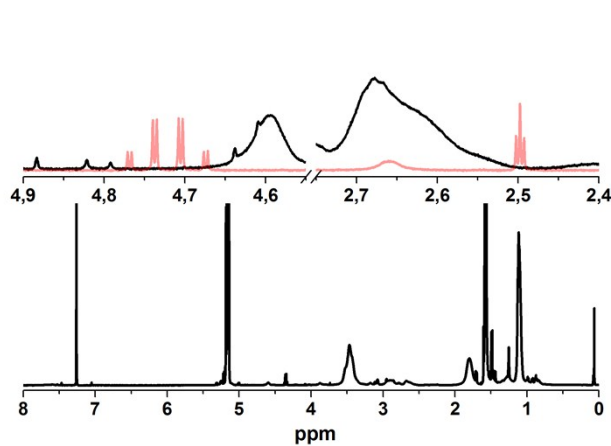
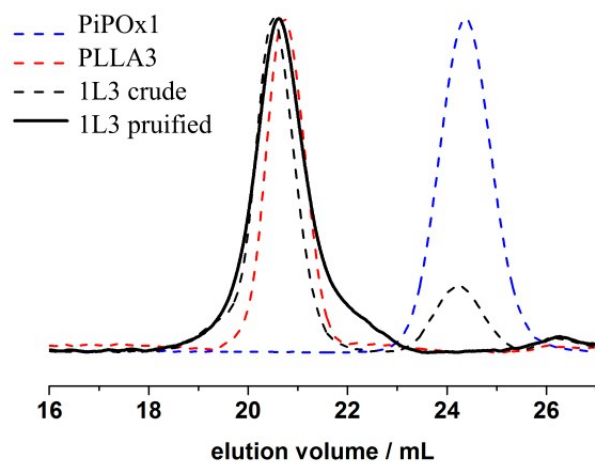
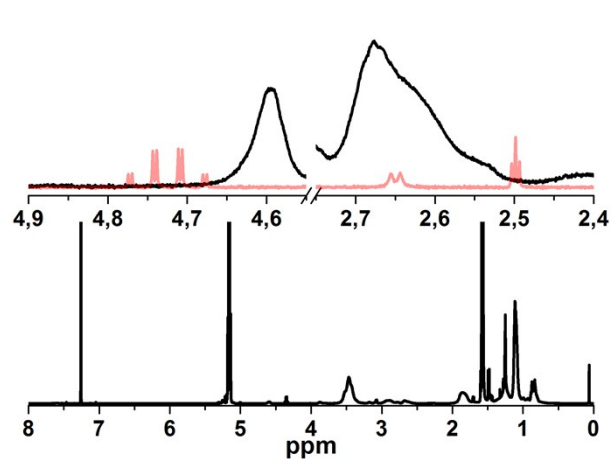
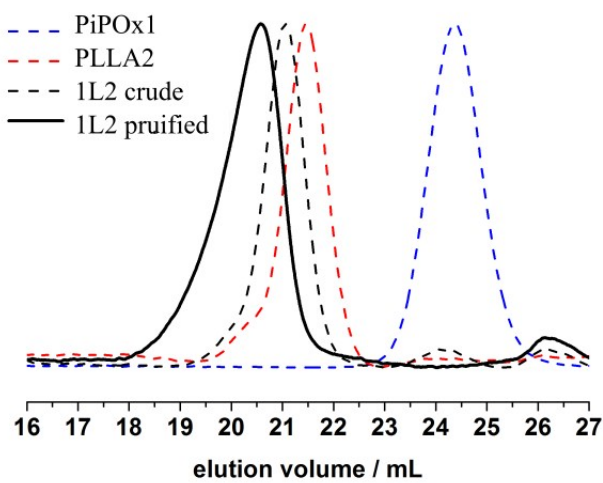
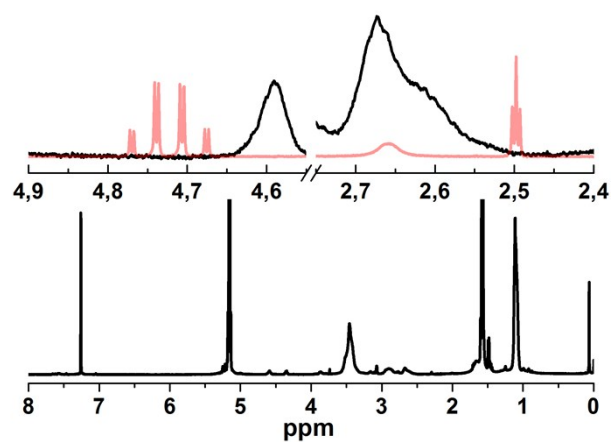
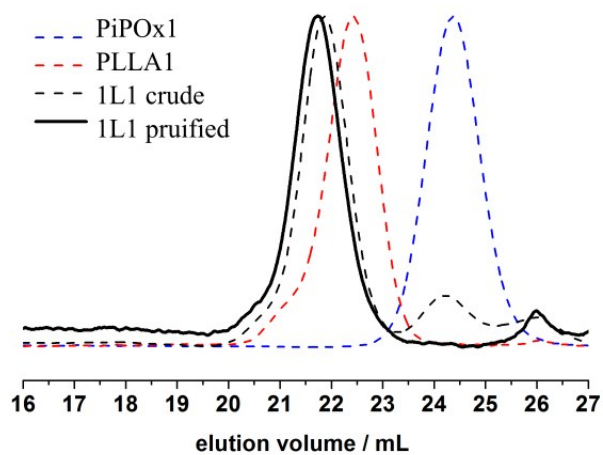
Supporting information



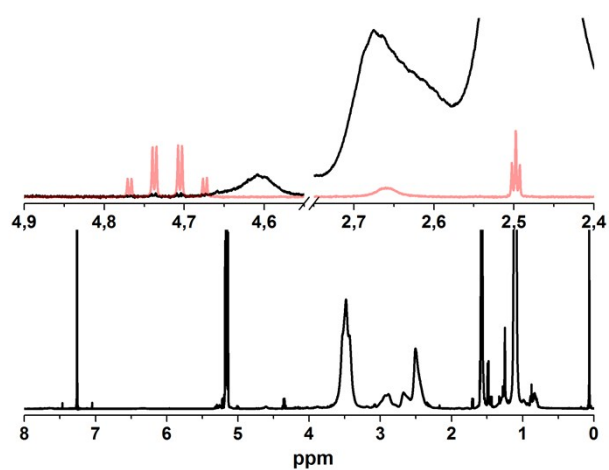
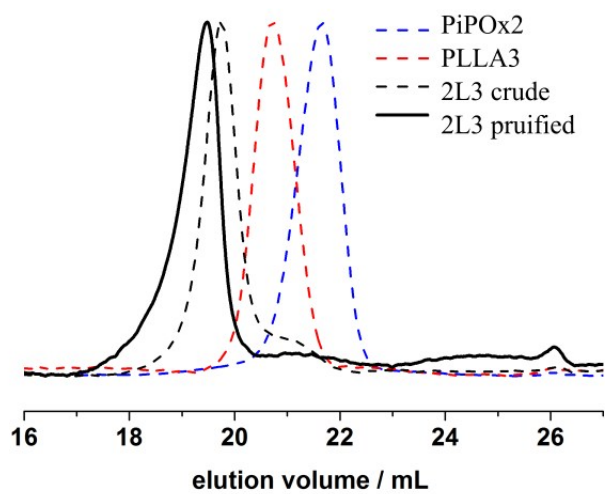
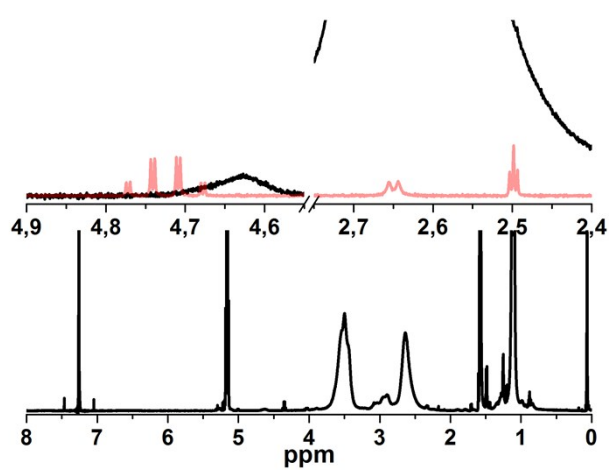
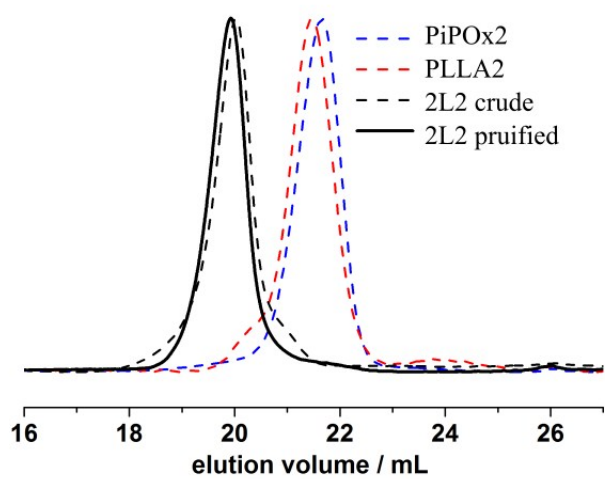
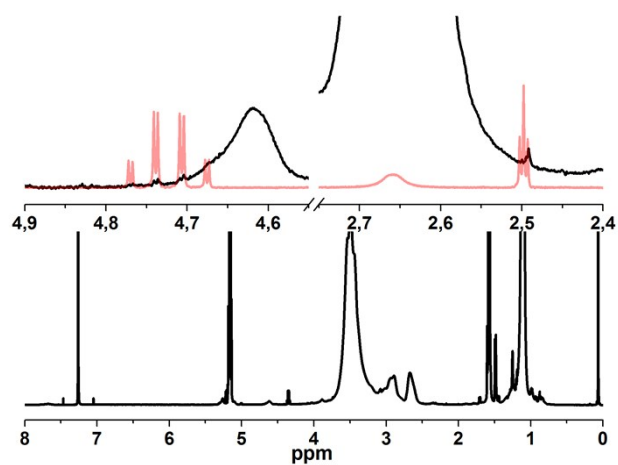
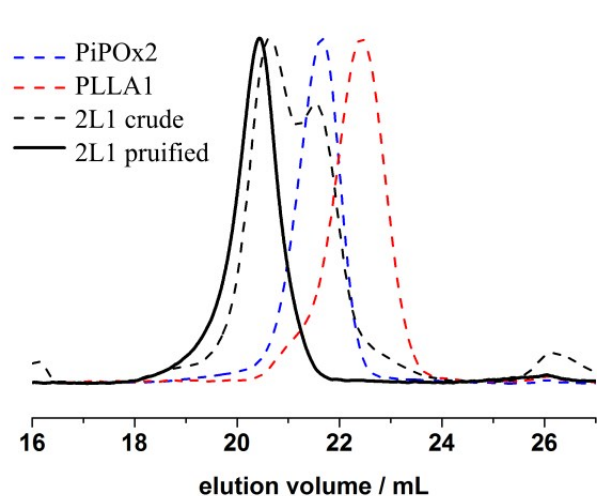
Supporting information



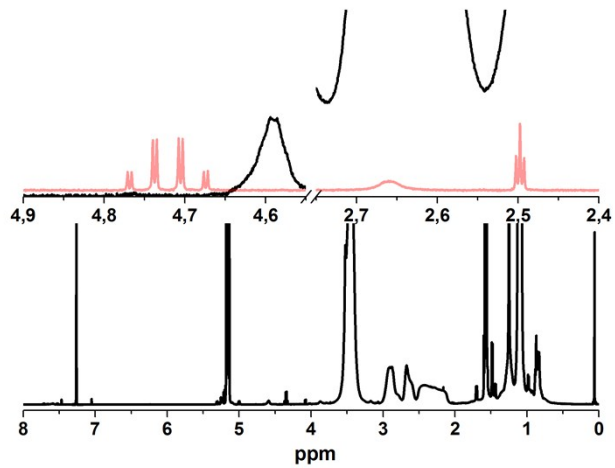
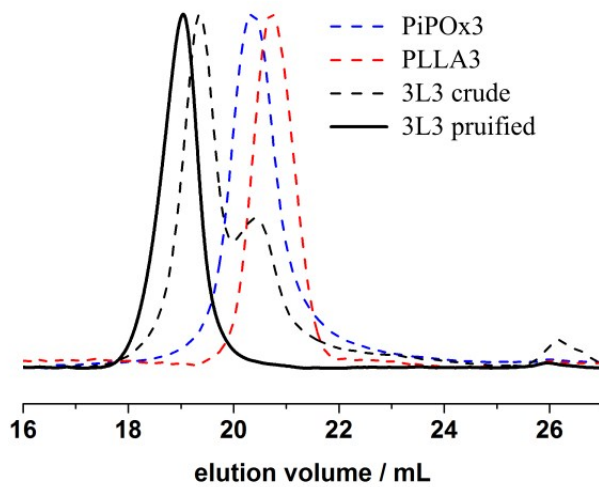
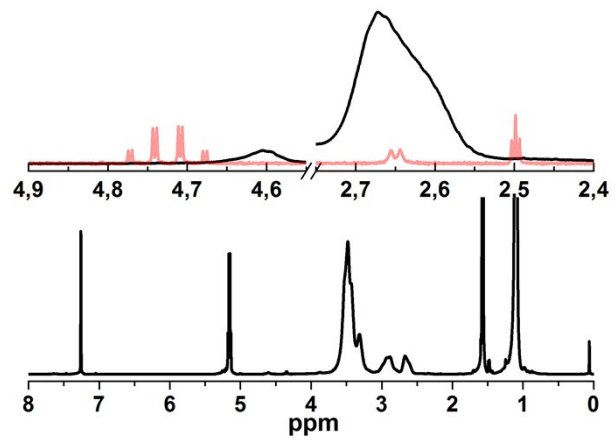
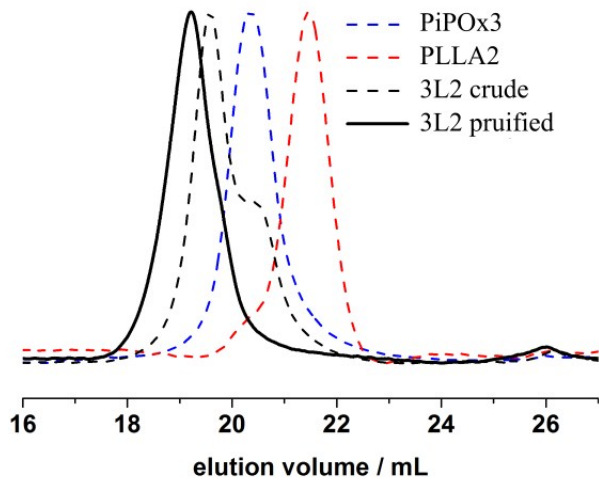
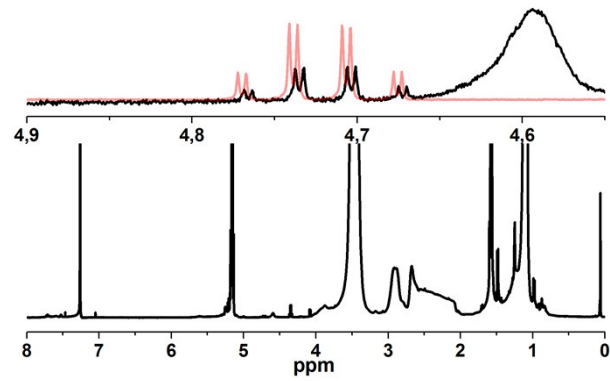
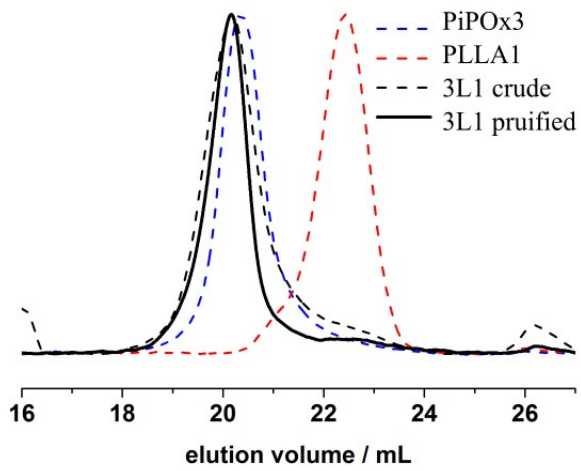
Supporting information



Supporting information



Supporting information



Supporting information

Figure S4 (Left) SEC traces of the block copolymers, their parent homopolymers and the crude reaction mixture. (Right) ¹H-NMR of the BCPs. The expansions show the disappearance of the propargyl signals.

2) Calculation of solubility parameters

The solubility parameters $\delta_{\text{PiPOX}} = 24.0 \text{ J}^{0.5}/\text{cm}^{1.5}$ and $\delta_{\text{PLA}} = 22.7 \text{ J}^{0.5}/\text{cm}^{1.5}$ were calculated according to Fedors' method (equation S1).⁶ δ^2 is the cohesive energy density (CED), defined as the molar energy

(ΔE_v) of vaporization per unit volume (V). $\sum_i \Delta e_i$ and $\sum_i v_i$ are the sums of atomic and group contributions to the CED (Table S2). The polymer end-groups were neglected.

$$\delta = \left(\frac{\Delta E_v}{V}\right)^{0.5} = \left(\frac{\sum_i \Delta e_i}{\sum_i v_i}\right)^{0.5} \quad (\text{Equation S1})$$

Table S2 Group contributions to the CED

Group	$\Delta e_i / \text{J/mol}$	$v_i / \text{cm}^3/\text{mol}$
CH ₃	4707	33.5
CH ₂	4937	16.1
CH	3431	-1.0
CON (tert. amide)	29497	-7.7
CO ₂ (ester)	17991	18.0

3) T_g regions of all BCPs

Supporting information

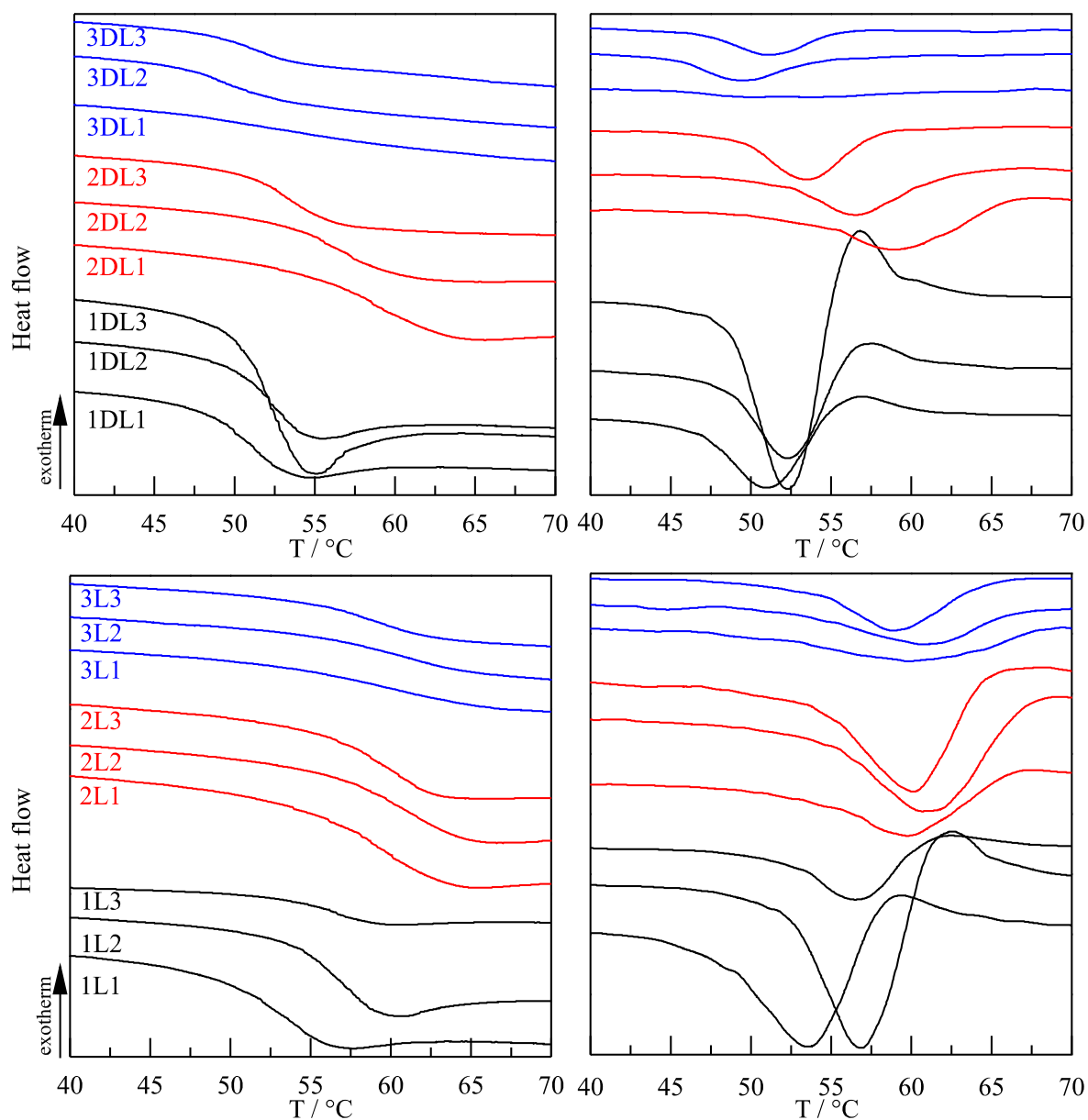


Figure S5 (left) DSC heating scan (10 °C/min) in the T_g region of the BCPs and (right) the first derivative of the respective curves.

4) Detailed crystallization properties of the homopolymers

The crystallization kinetics of PLLA and PiPOx exhibited an opposed molecular weight dependence. At a cooling/heating rate of 10 °C/min (Figure S6) the PLLA homopolymers crystallized during the cooling scan (T_c : 104 – 114 °C) and no crystallization was observed during the subsequent heating scan. T_c , T_m , ΔH_c and ΔH_m (Table S3) increased with the molecular weight. Also the equilibrium melting temperature T_m° increased with increasing molecular weight (Figure S7).

Supporting information

T_m° refers to a crystal with infinite thickness and can be obtained by extrapolation of the T_m vs T_c data after isothermal crystallization at various temperatures to the line $T_c = T_m$.⁷ The rationale behind this treatment is the increasing crystal thickness with T_c leading to higher experimental T_m . T_m° is an important thermodynamic parameter as it defines the driving force for crystallization (degree of undercooling, $\Delta T = T_m^\circ - T_c$) at a given T_c .

The crystallization rates of the homopolymers are depicted in Figure S7 in terms of the inverse crystallization half times $\tau_{1/2}^{-1}$ as a function of T_c . $\tau_{1/2}$ is the time at which 50 % of the crystallization process is completed and measured by isothermal DSC experiments. Plots of $\tau_{1/2}^{-1}$ vs T_c are expected to show a symmetric bell-shaped function centered on the $T_{c,max}$ of highest crystallization rate and T_g and T_m° as lower and upper limits. Increasing T_c from $T_{c,max}$ reduces the crystallization rates due to a lower degree of undercooling, decreasing the T_c reduces the crystallization rates due to limited chain mobility. We observe for the PLLA homopolymers of this study 1) an increasing maximum crystallization rate with decreasing molecular weight and 2) a decreasing $T_{c,max}$ with decreasing molecular weight. The first observation is known from literature and is explained by the exponential drop of intrinsic viscosity with the decrease of molecular weight.⁸ Accordingly, the chain mobility increases and allows faster diffusion to the crystal front. The second observation is due to the decreasing T_m° with decreasing molecular weight. The lower temperature side of the bell-shaped curve was not accessible for PLLA as the samples would start to crystallize during the cooling process before the isothermal temperature was reached.

In comparison to PLLA the maximal crystallization rates of the PiPOx homopolymers were dramatically lower (Figure S7) indicating entirely different requirements for crystallization and crystallization mechanisms. In addition we observed a strong molecular weight dependence of the crystallization behavior of PiPOx. At a cooling rate of 10 °C/min from the melt (Figure S6) PiPOx3 showed a strong exotherm (ΔH_c : 31.7 J/g) compared to PiPOx2 (ΔH_c : 2.0 J/g). Both PiPOx3 and PiPOx2 exhibited cold crystallization during the subsequent heating (ΔH_{cc} : 2.0 J/g and 14.9 J/g, respectively). Altogether, the crystallization of PiPOx2 was incomplete compared to PiPOx3, reflected by the reduced melting endotherm (23.2 J/g and 33.2 J/g, respectively). PiPOx1 remained amorphous during the entire experiment. T_m° of PiPOx2 and PiPOx3 were similar (203 and 205°C, respectively) but T_m° of PiPOx1 was strongly reduced (149 °C) shifting its crystallization window to lower temperatures. Unlike PLLA, the crystallization rate maximum of PiPOx increased with the molecular weight. It has been speculated earlier that the crystallization of PiPOx resembles typical features of the self-assembly of liquid-

Supporting information

crystalline polymers.^{9,10} These polymers undergo a series of concerted side-chain and main-chain conformational changes before transforming into the liquid crystalline phase.¹¹ Already the first reports of poly(alkyloxazolines) note the parallel orientation of a slightly distorted polymer backbone during crystallization.¹² Later it was reported that the backbone in the crystalline state is fully extended without any chain folding.¹³ The chemical structure of the repeating unit facilitates the packing of polymer due to high symmetry. The amide renders a coplanar system of side-groups without stereo-centers. Subsequent side-groups are alternating laterally due to the backbone structure. In summary, a directional growth mechanism of the crystalline phase due to oriented dipolar interactions was proposed.¹³ It can be rationalized that the increased crystallization rates of PiPOx with increasing molecular weights are due to the sum of oriented dipoles along one chain. Reducing the chain length increases the defects of dipole orientation and slows down the crystallization.

The crystallization of PLLA appears to be diffusion limited while the crystallization of PiPOx requires a series of conformational changes resulting in additive dipole orientation.

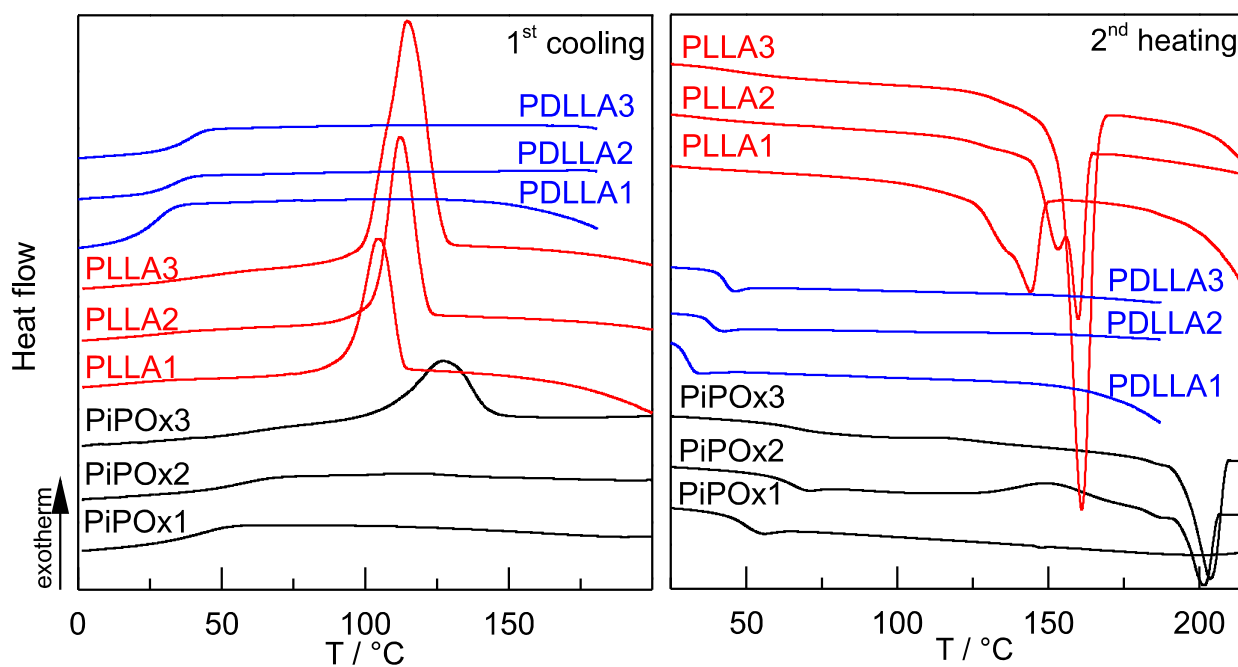


Figure S6 DSC cooling and heating scans (10 °C/min) of the homopolymers

Supporting information

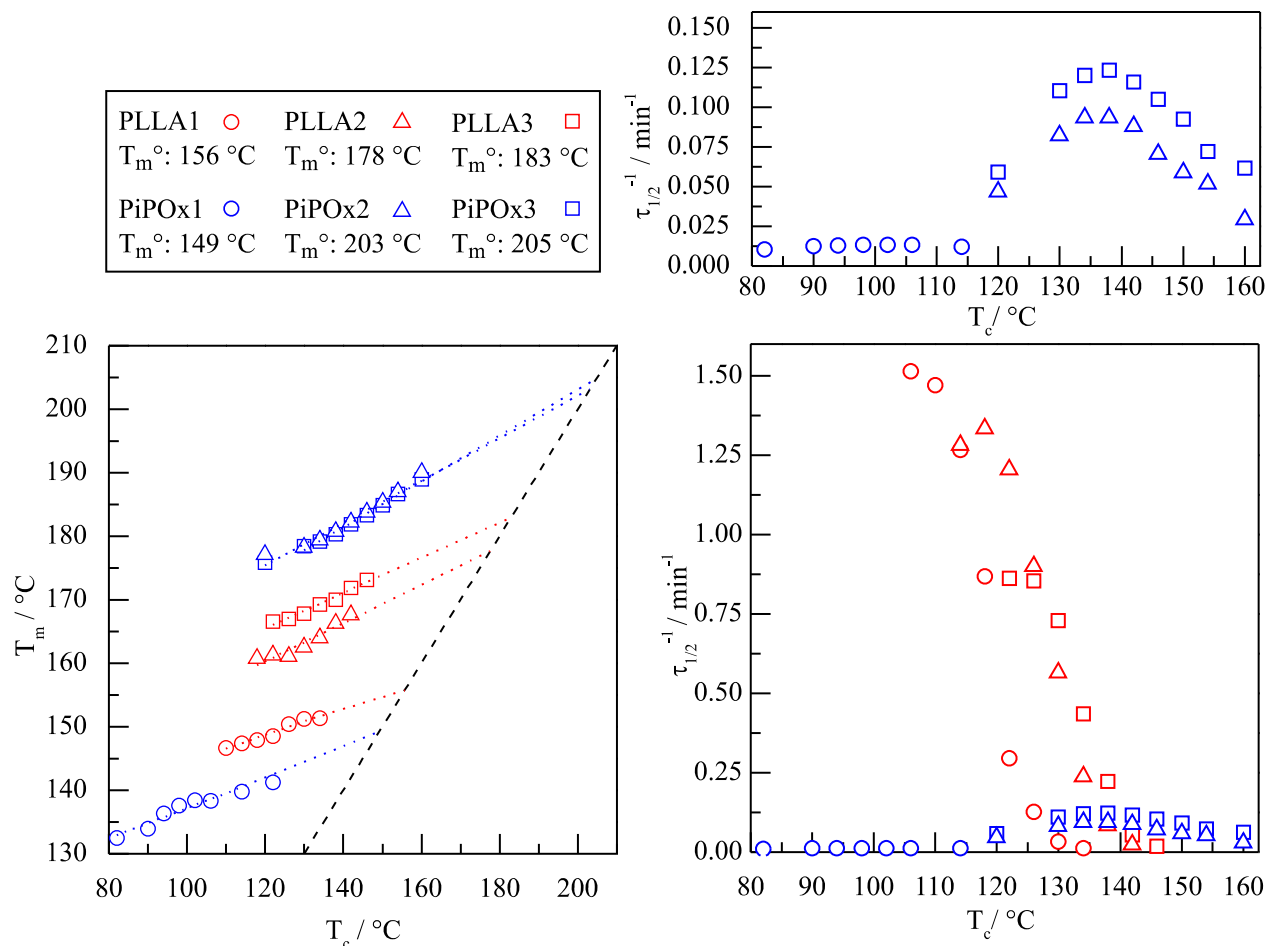


Figure S7 (left) Hoffman-Weeks plot gives the equilibrium melting temperatures T_m° of the PLLA and PiPOx homopolymers by extrapolation of the T_m vs T_c data to the $T_m = T_c$ line, (right) crystallization rates expressed as inverse crystallization half-times $\tau_{1/2}^{-1}$ vs crystallization temperature of the PLLA and PiPOx homopolymers, the top panel is an expansion of the PiPOx data.

Table S3 Thermal transitions of all homo- and diblock copolymers during DSC scans with a rate of $10^\circ\text{C}/\text{min}$

Polymer	1 st cooling			2 nd heating					
	T_c	ΔH_c^a	T_g	T_{cc}	ΔH_{cc}^a	$T_{m, PLLA}$	$\Delta H_{m, PLLA}^a$	$T_{m, PiPOx}$	$\Delta H_{m, PiPOx}^a$
PiPOx1	-	-	50.0	-	-	-	-	-	-
PiPOx2	119.2	2.0	64.3	150.5	14.9	-	-	202.0	-23.3
PiPOx3	127.3	31.7	66.3	117.2	2.0	-	-	203.7	-33.2
PLLA1	104.4	45.5	45.3 ^c	-	-	143.4	-44.1	-	-
PLLA2	112.1	51.9	51.9 ^c	-	-	160.0	-46.9	-	-
PLLA3	114.5	54.1	51.8 ^c	-	-	161.2	-62.3	-	-
PDLLA1	-	-	30.4	-	-	-	-	-	-
PDLLA2	-	-	37.7	-	-	-	-	-	-
PDLLA3	-	-	42.6	-	-	-	-	-	-
IDL1	-	-	51.3	-	-	-	-	-	-

Supporting information

1DL2	-	-	52.2	-	-	-	-	-	-
1DL3	-	-	52.3	-	-	-	-	-	-
2DL1	-	-	58.5	145.3	10.3	-	-	197.2	-12.8
2DL2	109.3	4.0	57.3	142.3	20.6	-	-	197.4	-23.3
2DL3	112.2	8.6	52.8	137.1	23.6	-	-	197.5	-46.7
3DL1	123.4	36.8	50.6	-	-	-	-	202.6	-36.9
3DL2	124.6	34.3	49.2	-	-	-	-	202.9	-37.2
3DL3	137.2	38.8	50.9	-	-	-	-	205.1	-34.7
1L1	-	-	54.4	-	-	-	-	-	-
1L2	-	-	57.0	131.4	19.1	150.0	-27.9	-	-
1L3	-	-	56.6	122.9	43.8	^d	^d	-	-
2L1	109.6	11.6	60.0	124.8	21.4	-	-	197.4	-39.4
2L2	-	-	61.6	142.7	27.4	-	-	199.6	-28.5
2L3	113.4	2.8 ^b	60.5	122.2	19.7 ^b	158.7	-47.1	198.3	-19.8
3L1	118.2	29.3	60.7	117.6	6.3	-	-	202.0	-35.1
3L2	124.2	31.5	61.3	-	-	-	-	202.6	-34.7
3L3	126.5	40.0	58.1	93.9	4.8	143.8	-17.3	203.3	-41.7

^a ΔH values were corrected by the weight fraction of the respective blocks; ^b ΔH values were not corrected, due to unclear assignment; ^c Obtained from the 1st heating cycle of a melt quenched sample; ^d two melting endotherms: 149.8 °C (11.2 J/g) and 156.8 °C (37.8 J/g).

5) Isothermal crystallization of 2L3

To confirm the crystallization driven phase-separation mechanism and consecutive crystallization of PiPOx and PLLA in 2L3 two isothermal experiments at 130 °C were conducted (Figure S8). In the first experiment the sample was kept at 130 °C for 2 h. The heat flow is exothermic and peaks at 4 min. Crystallization continues for 20 min although at a much lower heat flow. The two chronologically separated events are the crystallization of PiPOx and PLLA. The following heating scan exhibits the melting peaks of both PLLA (152 °C) and PiPOx (198 °C). In the second experiment isothermal crystallization was stopped after 4 min and the following heating curve exhibits only the melting of PiPOx.

Supporting information

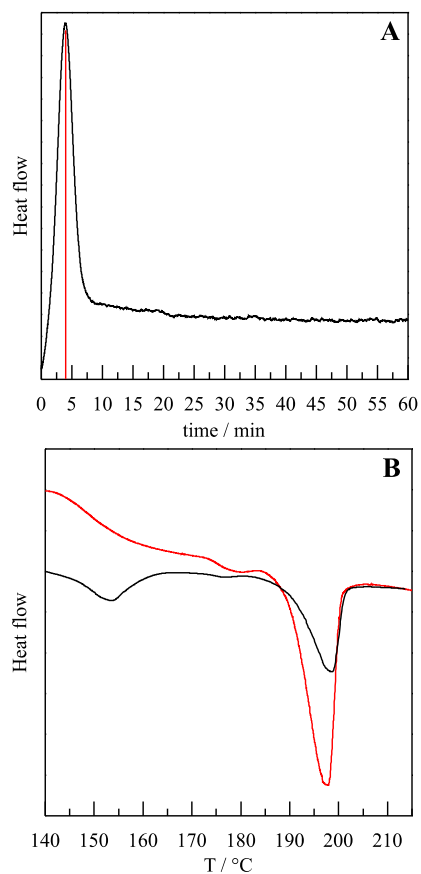


Figure S8 (A) Heat flow during the isothermal crystallization of 2L3 at 130 °C, the red line indicates a period of 4 min. (B) Heating curves of 2L3 after isothermal crystallization at 130 °C for 2 h (black) and 4 min (red).

6) Isothermal crystallization raw data

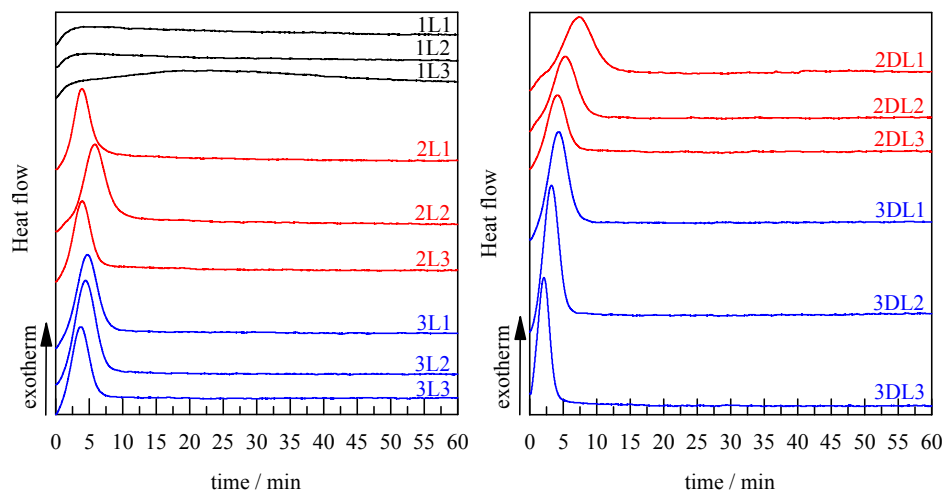


Figure S9 Heat flow during the isothermal crystallization of the indicated BCPs at 130 °C.

7) References

- 1 H. Witte and W. Seeliger, *Justus Liebigs Ann. Chem.*, 1974, **1974**, 996–1009.
- 2 R. Hoogenboom, *Angew. Chem. Int. Ed.*, 2009, **48**, 7978–7994.
- 3 Y. Li, J. N. Hoskins, S. G. Sreerama and S. M. Grayson, *Macromolecules*, 2010, **43**, 6225–6228.
- 4 C. Weber, R. C. Becer, A. Baumgaertel, R. Hoogenboom and U. S. Schubert, *Des. Monomers Polym.*, 2009, **12**, 149–165.
- 5 A. Kowalski, J. Libiszowski, A. Duda and S. Penczek, *Macromolecules*, 2000, **33**, 1964–1971.
- 6 R. F. Fedors, *Polym. Eng. Sci.*, 1974, **14**, 147–154.
- 7 H. Marand, J. Xu and S. Srinivas, *Macromolecules*, 1998, **31**, 8219–8229.
- 8 P. Pan, W. Kai, B. Zhu, T. Dong and Y. Inoue, *Macromolecules*, 2007, **40**, 6898–6905.
- 9 S. Sun and P. Wu, *Phys. Chem. Chem. Phys.*, 2015, **17**, 31084–31092.
- 10 S. Sun, H. Tang, P. Wu and X. Wan, *Phys. Chem. Chem. Phys.*, 2009, **11**, 9861–9870.
- 11 Y. Shen, E. Chen, C. Ye, H. Zhang, P. Wu, I. Noda and Q. Zhou, *J. Phys. Chem. B*, 2005, **109**, 6089–6095.
- 12 M. Litt, F. Rahl and L. G. Roldan, *J. Polym. Sci. Part -2 Polym. Phys.*, 1969, **7**, 463–473.
- 13 A. L. Demirel, M. Meyer and H. Schlaad, *Angew. Chem. Int. Ed.*, 2007, **46**, 8622–8624.